Office de la Propriété Intellectuelle du Canada
Un organisme d'Industrie Canada

Canadian Intellectual Property Office
An agency of Industry Canada

CA 2446663 A1 2005/04/24

(21) 2 446 663

(12) DEMANDE DE BREVET CANADIEN
CANADIAN PATENT APPLICATION

(13) A1

(22) Date de dépôt/Filing Date: 2003/10/24

(41) Mise à la disp. pub./Open to Public Insp.: 2005/04/24

(51) Cl.Int.^{7}/Int.Cl.^{7} A61B 17/56, A61B 17/58, A61N 5/06

(71) Demandeur/Applicant:
UNIVERSITY HEALTH NETWORK, CA

(72) Inventeur/Inventor:
BURCH, SHANE, CA

(74) Agent: BERESKIN & PARR

(54) Titre : INSTRUMENT ET METHODE DE TRAITEMENT DES OS
(54) Title: BONE-TREATMENT INSTRUMENT AND METHOD

(57) Abrégé/Abstract:
Photodynamic therapy (PDT) is used to treat bone. A photosensitizing drug is administered to a mammal. Non-thermal light at a specific wavelength is delivered to a site adjacent or in bone to activate the drug. A cannulated bone screw is secured into bone. A fiber optic cable sheath extends from within the screw and is accessible. A fiber optic cable is inserted in the fiber optic cable sheath to deliver light to the bone. The light activates the drug. The cannulated bone screw and the fiber optic cable sheath may remain inside the mammal for further photodynamic therapy.

ABSTRACT OF THE DISCLOSURE

Photodynamic therapy (PDT) is used to treat bone. A photosensitizing drug is administered to a mammal. Non-thermal light at a specific wavelength is delivered to a site adjacent or in bone to activate the drug. A cannulated bone screw is secured into bone. A fiber optic cable sheath extends from within the screw and is accessible. A fiber optic cable is inserted in the fiber optic cable sheath to deliver light to the bone. The light activates the drug. The cannulated bone screw and the fiber optic cable sheath may remain inside the mammal for further photodynamic therapy.

B&P File No. 10723-69

BERESKIN & PARR

CANADA

Title: **BONE-TREATMENT INSTRUMENT AND METHOD**

Inventor: **Shane BURCH**

Title: Bone-Treatment Instrument and Method

FIELD OF THE INVENTION

[0001] This invention relates generally to treatment of bone, bone tumors and lesions, and diseases of the bone.

BACKGROUND OF THE INVENTION

[0002] Approximately 1.3 million cases of cancer were diagnosed in North America in 2001. Over 50% of these have the potential to metastasize to bone [14]. Each year, over one hundred thousand bone metastases are identified. Post-mortem autopsy results from patients with primary cancer indicate that 60% of spines examined had metastatic lesions. An estimated twenty to forty thousand cases of metastatic breast cancer lesions alone occur in the spine each year [1,2]. Metastatic lesions to the spine result in intractable back pain, loss of bowel and bladder function, paresis and paralysis. The lesions can affect singular or multiple vertebral bodies.

[0003] In the ambulatory patient the mainstay of treatment is radiation therapy, while surgery is reserved for those experiencing collapse or neurological compromise. Unfortunately radiation therapy provides only limited relief from pain, does not provide stability to the spine and adversely affects the soft tissue such that the morbidity and mortality of surgical intervention is increased threefold [3,4,5]. Results of radiation therapy for the treatment of spinal metastases have shown that only one third have complete relief of their back pain [15]. Radiation therapy is limited by the number of times it can be administered as it affects the integrity of the soft tissues and can induce radiation myelopathy. As the longevity of patients with spinal metastases increases (average survival 2 years with breast cancer, mean 1 year survival of 78%) [16] so does the likelihood of lesion recurrence and the necessity for spinal surgery. Recurrence with radiation therapy is estimated to be 33% [1,17]. Spinal surgery for patients with spinal metastases carries a 30 – 40% risk of morbidity and a 7 – 16% risk of mortality.

[0004] Photodynamic therapy (PDT) can directly target lesions. PDT ablates tissue with a non-thermal specific wavelength of light delivered to the targeted tissue. A photosensitizing drug is administered prior to the light. The light stimulates the drug to release energy which is toxic to the surrounding tissue [8,18] [19,20]. There are reports that the drug is preferentially taken up and retained in tumor tissue compared to normal tissue [21,22] making the treatment somewhat specific. This therapy has been used in lung [9,10], intraperitoneal [11] and prostate cancer [12].

[0005] There are several photosensitizing drugs now available with minimal systemic side effect profiles. Benzoporphyrin derivative monoacid ring A (BPD-MA) is a photosensitizer that can be used to either target the neo-vasculature or produce intracellular cytotoxic effects based on the drug-light interval [6,7,23,24,25,26]. The vascular targets are primarily affected if the drug light interval is short (15 minutes or less) while the intracellular effects are seen in tissue if the drug light interval is long (3 hours) [6,24]. There are several reports of its use in soft tissue tumors in the murine model [20,23,25,27] as well as of its use in an orthotopic chondrosarcoma [6] and fibrosarcoma tumor models [24,26]. Results from these studies showed a significant effect at both the 15 minute and 3 hour drug light interval was achieved with 33% of the lesions being completely ablated at 4 weeks post treatment. The greatest effect was seen with the shorter interval demonstrating the potency of BPD-MA to affect the neo-vasculature.

[0006] To date, there have not been any published reports of the use of this therapy in bone or in the spine. To date, there have not been any published reports of PDT use in an *in vivo* metastatic breast cancer model affecting bone. To date, there have not been any published reports of the pharmacokinetics of BPD-MA for bone. There is a paucity of literature on the optical properties of bone.

[0007] Takeuchi et al., 1997 [28], reported on the optical properties of cancellous and cortical bone in comparison to muscle, fat and saline. Cortical bone has a high attenuation to light while cancellous bone does not.

BRIEF DESCRIPTION OF THE DRAWINGS

[0008] For a better understanding of the present invention, and to show more clearly how it may be carried into effect, reference will now be made, by way of example, to the accompanying drawings which show some embodiments of the present invention, and in which:

FIGURE 1 shows stereotactic targeting of bioluminescent metastatic lesions in a rat using a mini-C-arm image intensifier;

FIGURE 2 shows the *in vitro* uptake of BPD-MA in MT-1 cells;

FIGURE 3 is a plot of the BPD-MA drug uptake in serum and spinal cord of the nude rat;

FIGURE 4 shows fluorescence microscopy of BPD-MA uptake in the spinal cord and vertebrae of the nude rat;

FIGURE 5 is a bar graph of the *in vitro* cell viability following BPD-MA PDT;

FIGURE 6 is a high definition radiographic (Faxitron) lateral view of rat vertebrae and femur at 21 days post left intracardiac tumor injection;

FIGURE 7 shows micro-CT analysis of rat vertebrae 21 days following intracardiac injection of MT-1 cells;

FIGURE 8 shows micro-CT analysis of rat tibia 21 days following intracardiac injection of MT-1 cells;

FIGURE 9 shows histological and immunohistochemical staining of MT-1 cells within vertebrae;

FIGURES 10 and 12 show pre and post-PDT treatment bioluminescent imaging of MT-1luc+ metastatic lesions in rnu/rnu rats with BPD-MA;

FIGURE 11 is a bar graph of the effect of PDT on bioluminescent tumor in rats;

FIGURE 13 is a photograph of light passing through a human cadaver vertebrae;

FIGURE 14 shows brightfield microscopy of H&E sections containing tumor following PDT treatment;

FIGURE 15 shows brightfield microscopy of rat vertebrae following PDT treatment;

FIGURE 16 shows an inserted guide pin and the insertion of another guide pin with a cannulated drill;

FIGURE 17 shows an inserted cannulated exchange sheath and the insertion of a cannulated bone screw assembly;

FIGURE 18 shows an expanded view of a cannulated exchange sheath, a cannulated bone screw, a flexible O-ring and a cannulated locking screw;

FIGURE 19 shows inserted fibre optic cable sheaths and inserted fiber optic cables;

FIGURES 20 and 21 show a vertebrae with a bone screw in place and a fiber optic probe inserted;

FIGURES 22 and 23 are graphs showing some of the results of the light attenuation studies in bone;

FIGURE 24 shows some of the equipment used in the *in vivo* pig study;

FIGURE 25 is a drawing of an example of the cannulated bone screw; and

FIGURE 26 is a drawing of an example of the cannulated locking screw.

DETAILED DESCRIPTION OF EMBODIMENTS OF THE INVENTION

[0009] In some embodiments of the invention, photodynamic therapy (PDT) is used in bone. The method involves administering a photosensitizing drug to a mammal having bone tumors or other bone disease. A "bone tumor" refers to a primary or metastatic tumor associated with bone, that is, a tumor on or in a bone. A non-exhaustive list of photosensitizing drugs includes benzoporphyrin derivative monoacid ring A (BPD-MA) (also known as verteporfin and Visudyne®), palladium-bacteriopheophorbide (known as TOOKAD®), and 5-aminolaevulinic acid (ALA). Non-thermal light of a specific wavelength suitable for stimulating the photosensitizing drug is applied to the bone. The photosensitizing drug may target the neo-vasculature and/or produce intracellular cytotoxic effects and/or inhibit growth of or destroy the tumor cells in some other, yet to be elucidated, manner.

[0010] For small bones a fiber optic cable is inserted into the mammal and placed adjacent a bone lesion. For larger bones such as, for example, pig and human vertebrae, a cannulated bone screw is secured into the bone. The cannulated bone screw has a head, an externally-threaded shaft and a frustro-conical tip. A fiber optic cable sheath is located inside the cannula of the screw and extends from the tip of the bone screw beyond the screw to at least the skin of the mammal. Photodynamic therapy can be used on one or more occasion by administering a photosensitizing drug, inserting a fiber optic cable into the fiber optic cable sheath, and delivering the light through the fiber optic cable. The bone screw and the fiber optic cable sheath remain in place from one PDT treatment to the next. Once it has been decided not to use PDT treatment at the site of the bone screw anymore, the fiber optic cable sheath is removed and bone cement is injected through the bone screw to stabilize the deteriorated bone.

[0011] The results of *in vitro* studies indicated that cells from a human metastatic breast cancer cell line (MT-1) were susceptible to PDT with BPD-MA while the cells were not sensitive to the drug or the light individually. This is consistent with reports in the literature [23,29]. Furthermore, uptake into

MT-1 cells was demonstrated directly with real time fluorescent microscopy indicating that these cells were susceptible to intracellular cytotoxic effects of PDT.

[0012] *In vivo* studies in a rat model demonstrated the effectiveness of PDT on bone tumors from a human metastatic breast cancer cell line. A bioluminescent metastatic model in the nude rat was developed to facilitate the localization and targeting of the lesions.

[0013] As part of these studies, the drug uptake studies indicated that the spinal cord had minimal uptake of BPD-MA suggesting that it would not be susceptible to damage during treatment. The fluorescence microscopy however, indicated that BPD-MA is taken up into the spinal cord. Furthermore it showed that the drug has a delayed uptake (greater than 1 hour) and suggested that the optimal drug light interval prior to PDT would be less than 1 hour or greater than 24 hours.

[0014] The model used in this study was a purely metastatic model involving a human breast cancer cell line. Engebraaten and Fodstad, 1999, demonstrated lesions within all vertebrae and of *rnu/rnu* rats between 14 and 21 days [13]. In the inventor's studies, metastases occurred in the spine, long bones and lung. Fine detail radiography revealed lesions within long bones as early as 14 days post tumor injection. Rapid weight loss was seen after 18 days post injection followed by overt tumors in the mandible and distal femur and proximal tibia. Paralysis and death secondary to tumor burden occurred typically around day 21 and 23 respectively. Micro-CT scanning revealed multiple large lytic lesions within most vertebrae and long bones of affected animals. Subsequent histological analysis confirmed the presence of the tumor within the vertebrae and long bones and demonstrated the invasiveness of the tumor. The bioluminescence allowed determination of the growth of the lesions, location of the tumor and a way of targeting the tumor. In addition, bioluminescence has been shown to be quantitative in determining tumor ablation *in vitro* as well as *in vivo* [30,31]. Furthermore by imaging the tumor with bioluminescence, growth of the tumor could be

assessed, lesions could be detected early, then targeted and early treatment could be administered.

[0015] The *in vivo* results demonstrate the effectiveness of this therapy in treating a human metastatic breast cancer in both the vertebrae and long bones. The results indicate that PDT can ablate tumor tissue within bone and that the *in vivo* structure of bone and bone marrow is not a limiting factor for this therapy. The bioluminescent data indicated that a 99.8% reduction in tumor growth was obtained with one treatment. The largest area of effect had a diameter of 2.2 cm and was created by a 200um fiber optical cable with a treatment time of 16 minutes at 150 Joules. The results also indicate that the area of tumor ablated is directly proportional to the amount of light supplied to the targeted area. A shorter treatment time (3 minutes) produced a smaller effect than longer treatment times with a 66% reduction in the tumor growth with the 25J group. Based on work by Richter *et al.*, [22] in the mouse, the inventor hypothesized that 24 hour drug-light interval would be selective for tumor ablation. Yet, this was not the case. There was no difference between control animals and those animals treated with a 24 hour drug light interval with respect to ablation of tumor tissue.

[0016] The spinal cord in the rat is very sensitive to PDT as the drug is taken up into the cord by 3 hours. We anticipated that a window of opportunity would exist based on the delay of transport of the drug across the drug-spinal cord barrier, yet, even at short drug-light intervals when drug was not seen in the spinal cord by fluorescence microscopy, paralysis was seen. This suggests that in the rat model the PDT effect was vascular in nature while the spinal cord is also susceptible to cytotoxic damage as drug light intervals of 3 hours had an effect. Note that treatment with light only or drug only did not affect the tumor, bone, bone marrow or spinal cord. The nerve roots and peripheral nerves were not affected following treatment at the 3 hour drug light interval at any light dose. No paralysis was seen when treatment was administered with a 24 hour drug light interval.

[0017] In summary the results suggest that PDT with BPD-MA could be an effective treatment directed against metastatic tumors in bone. This treatment would be used preferentially to treat tumors within the vertebrae through a trans or para-pedicular approach and could be implemented to treat multiple vertebrae. The size of the lesions produced in the rat spine defined an area of effect that is well suited for lesions within human vertebrae. The area of effect can be varied easily allowing for safe operating parameters around the spinal cord. However, in larger vertebrae in which the fiber optic cable is implanted within the bone the inventor anticipates the effect on the spinal cord will be negligible. Studies in larger animals were required to establish the safety of this treatment in the spine.

[0018] Studies of light attenuation in human cadaver vertebrae demonstrated the feasibility of PDT in large bones. FIGURE 13 is a photograph from these studies.

[0019] *In vivo* studies in a pig model demonstrated the feasibility of a procedure using a cannulated bone screw to facilitate delivery of light to the bone and as a conduit to introduce bone cement to stabilize a large bone that has been deteriorated by its tumor load. The *in vivo* studies in the pig model also measured the attenuation of light within a vertebral body, and from the derived data, safe doses of light and drug were determined.

[0020] These studies, as well as a detailed description of the surgical procedure using the cannulated bone screw, will now be described in more detail.

***In vitro* studies**

[0021] *In vitro* uptake of BPD-MA in MT-cells:

Method: MT-1 cells, a human breast cancer cell line, provided courtesy of Dr. O. Engebraaten, Norwegian Radium Hospital, Oslo, Norway, were grown and maintained in RPMI media containing penicillin and streptomycin with 10% fetal bovine serum at 37 degrees Celsius. Once the cells had reached subconfluence they were resuspended in free RPMI. The cells were

harvested using a 0.05% trypsin –0.05mM EDTA solution. Cells were then counted with a hemocytometer and plated at $2x10^5$ cells/ml in an inverted microscopy slide chamber in PBS. BPD-MA was then added to the suspension at a concentration of 1 ug/ml. The cells were then visualized under bright field and fluorescence microscopy (Zeiss Axiophot) using an excitation/emission filter of 490 nm/ nm emission respectively. Uptake of drug into the cells was monitored overtime using live video photography with a CCD camera attached to the microscope.

Results: FIGURE 2 shows the *in vitro* uptake of BPD-MA in MT-1 cells. A) is a bright field microscopy image of MT-1 cell (63x) and C) is an overlay of the bright field and fluorescent image showing colocalization of BPD-MA within MT-1 cells (63x). The MT-1 cells began fluorescing at 45 minutes following incubation with BPD-MA.

[0022] PDT effect on *in vitro* MT-1 cells:

Method: MT-1 cells were grown and maintained in RPMI media containing penicillin and streptomycin with 10% fetal bovine serum at 37 degrees Celsius. Once the cells had reached subconfluence they were resuspended in free RPMI. The cells were harvested using 0.05% trypsin –0.05 mM EDTA solution. Cells were then counted with a hemocytometer and plated at $2x10^5$ cells/ml in a 96 well plate. BPD-MA was then added to the individual wells at a concentration of 1 ug/ml or 10 ug/ml. 690 nm light was administered at 150 mW to the individual wells at a fluence of either 100 J/cm^2 or 25 J/cm^2 following an 8 hour incubation period. Control wells included those that did not contain cells, those that contained cells but no BPD-MA, those that contained cells and drug but did not receive a light does and those that contained cells and received a light dose but were not incubated with BPD-MA. Following treatment the cells were allowed to survive for 24 hours following which a sulpharodamine bromide (SRB) assay was performed to establish the number of viable cells remaining. Briefly, cells were fixed in 10% trichloroacetic acid and stained with a sulpharodamine bromide solution

selectively staining viable cells. A spectrophotometer was then used to assess the absorbance of 540 nm light within individual wells of the 96 well plate which was correlated to the number of remaining cells following treatment.

Results: The effect of PDT on *in vitro* MT-1 cells was demonstrated using a SRB assay. A significant difference was seen between the absorbance in the untreated wells versus the wells treated with light and drug. No significant difference was seen between untreated wells and wells treated with light only or drug only (Table 1). As shown in FIGURE 5, there was no difference between the two drug concentrations (10 ug/ml and 1 ug/ml BPD-MA) with respect to the treatment group and there was no significant difference in absorbance between BPD-MA wells treated with either 100 J/cm^2 or 25 J/cm^2.

Table 1a. SRB Assay

Group	Drug Dose	Light Dose	Standard Mean (absorbance)	Standard Deviation	95% Confidence Interval
1	1ug/ml x	200J/cm^2	.2923	.0794	**.2419**
2	1ug/ml x	25J/cm^2	.1946	.0618	**.1553**
3	10ug/ml x	200J/cm^2	.2558	.0865	**.2009**
4	10ug/ml x	25 J/cm^2	.2049	.0523	**.1717**
5	No cells	No cells	.0206	.0269	**.0035**
6	/	200J/cm^2	1.4954	.2884	**1.3122**
7	1ug/ml	/	1.2392	.3417	**.8806**
8	**Cells Only**	**Cells Only**	**1.5992**	**.2800**	**1.4212**

Table 1b. SRB Assay ANOVA with Bonferroni for multiple comparisons (* indicate significant difference between groups)

	Group	5	2	4	3	1	7	6	8
Group	**Mean**								
5	.0206								
2	.1946								
4	.2049								
3	.2558	*							
1	.2923	*							
7	1.2392	*	*	*	*	*			
6	1.4954	*	*	*	*	*			
8	1.5992	*	*	*	*	*	*		

***In vivo* studies in rat model**

[0023] BPD uptake in the serum and spinal cord:

Method: BPD-MA was administered to 10 rats (Sprague-Dawley, 150gm) through a tail vein injection. Animals were then sacrificed using $C0_2$ inhalation overdose at 16 minutes, 3 hrs, 6 hrs and 24 hrs following injection. Control animals without BPD-MA were euthanized in a similar fashion. Serum samples and spinal cord tissue samples were harvested from the animals at the time of euthanasia. A segment of spine was also fixed in 10% formalin for 7 days followed by decalcification for 7 days in 10% formic acid for fluoroscopic microscopic analysis. A control assay determined that BPD-MA fluorescence was not affected by formic acid. BPD-MA concentration within the serum and spinal cord tissue was then determined using fluorimetry. Briefly, the samples were solubilized and the samples were tested with excitation and emission spectra specific to BPD-MA. The fluorescence of the drug within the tissue was correlated to the specific uptake of the drug within the tissue. Fluorescent microscopy was also used to visualize the presence or absence of BPD-MA within the vertebrae and spinal cord at 1 hour, 3 hours and 24 hours.

Results: Fluorimetry was used to determine the specific uptake of the BPD in the spinal cord at 15 minutes, 3 and 24 hours post injection. As shown in FIGURE 3, the specific uptake studies indicated that there was rapid increase in the serum drug concentration over 15 minutes but began to decline after 3 hours and returned to baseline by 24 hours post injection. There was no apparent difference between samples from the spinal cord at 15 minutes, 3 hour and 24 hour intervals as compared to the control group. FIGURE 4 shows fluorescence microscopy of BPD-MA uptake in the spinal cord and vertebrae. A) shows the uptake of BPD-MA in the vertebrae at 15 minutes, B) shows the uptake of BPD-MA in the spinal cord at 15 minutes, C) shows the uptake of BPD-MA in the vertebrae at 3 hours, and D) shows the uptake of BPD-MA in the spinal cord at 3 hours. Sagittal and coronal sections from the Sprague-Dawley rat vertebrae examined under fluorescent microscopy

indicated that there was delayed uptake into the spinal cord with no drug being present at 1 hour, yet, at 1 hour the bone marrow contained signal. At 3 hours the spinal cord and bone marrow contained an intense signal with neuronal cell bodies being labeled within the cord. At 24 hours the fluorescence of the drug within the spinal cord and vertebrae returned to baseline levels.

[0024] Spinal metastases model:

Method: Ten nude rnu/rnu (Harlan) female rats (4-6 weeks of age) were used in this part of the study. The animals were injected with MT-1 cells, a human breast cancer cell line, provided courtesy of Dr. O. Engebraaten, Norwegian Radium Hospital (Oslo, Norway) who had previously shown [13] that injection of these cells into the left ventricle in 4 week old nude rats produced spinal and boney metastases in all animals injected. The cells were grown and maintained in RPMI media containing penicillin and streptomycin with 10% fetal bovine serum at 37 degrees Celsius. The protocol was in accordance with standards of the Canadian Council on Animal Care. The chest of each animal was then prepared with alcohol and 2 $x10^6$ cells of MT-1 were injected into the left ventricle using a 1 ml syringe with a 26g needle. Pulsatile blood in the syringe was ensured prior to each injection. The animals were placed back into their cages and fed water and rat chow ad libitum and kept on a constant light dark cycle. The animals were then imaged by fine detail radiography at 14 and 21 days post injection. The animals were examined for overt tumors, paralysis and cachexia following injection. The animals were sacrificed using CO_2 inhalation for compassionate reasons between day 23 and day 30 depending on individual tumor burden. Vertebrae and long bones were then harvested and fixed in 10% formalin for 7 days. Micro-CT images were obtained and then the samples were decalcified in 10% formic acid for 7 days. The tissue was then blocked, paraffin embedded and analyzed under light microscopy using H&E staining.

[0025] Establishment of a transfected human breast cancer cell line expressing the luciferase gene:

Method: In brief, the MT-1 cells were grown and maintained in RPMI media containing penicillin and streptomycin with 10% fetal bovine serum at 37 degrees celcius. The MT-1 cells were then transfected with pCI-neo mammalian expression vector (Promega) using the Transfectam Reagent (Promega) transfection kit. Positive colonies were selected by adding 1000ug/ml G418 antibiotic (Promega) to the tissue culture media. Cell colonies with luciferase activity were identified using the Xenogen IVIS system (Alameda, California). Individual cells were then isolated from high photon emitting colonies and plated. The cells were then grown to subconfluence in RPMI media with antibiotics and 10% FBS in 1000 ug/ml of G418 antibiotic to ensure stable transfection.

[0026] Spinal Metastases Model and Establishment of a transfected human breast cancer cell line expressing the luciferase gene:

Results: Of the initial 10 animals injected with MT-1 cells 7 of the 10 animals developed metastatic disease. The mean survival of the animals with tumors was 25 days. Four of the animals showed palpable tumors in the femur and tibias as well as the lower mandible. Two animals developed hind leg paralysis secondary to metastatic disease. All animals with tumors became cachexic. The affected animals appeared well until day 18 after which the animals developed rapid weight loss and overt tumors.

High resolution radiography (Faxitron) indicated lesions within the humerus, femur and tibia as early as day 14 in some animals. For example, FIGURE 6 shows a lateral view of rat vertebrae and femur at 21 days post left intracardiac tumor injection. However, lesions could not be detected in the vertebrae of any animals by day 21 by high resolution radiography (Faxitron).

FIGURE 7 shows micro-CT analysis of rat vertebrae 21 days following intracardiac injection of MT-1 cells. The views are A) sagittal, B) transverse. C) shows coronal 3D reconstruction and D) shows sagittal 3D reconstruction.

Micro-CT analysis of the thoracic and lumbar spines of these animals showed multiple lytic lesions within the vertebrae. Similar lytic lesions were identified in the humerus, tibia and femur. FIGURE 8 shows micro-CT analysis of rat tibia 21 days following intracardiac injection of MT-1 cells. The views are A) sagittal, B) transverse. C) shows coronal 3D reconstruction and D) shows sagittal 3D reconstruction.

The mean area of the lytic lesions within the lumbar vertebrae was 2.92 mm^2 and 2.14 mm^2 in the thoracic vertebrae. The lesions approximated 1/3 of the vertebral body size in both the lumbar and thoracic vertebrae imaged, as summarized in TABLE 2.

Table 2. Vertebral Body Size and Tumor Size (microCT)

	Vertebral Body		Osteolytic Lesion (Tumor)	
	Sagittal (mm^2)	Coronal (mm^2)	Sagittal (mm^2)	Coronal (mm^2)
Lumbar *(n =3)*	9.4	7.09	2.92	2.3
Thoracic *(n = 3)*	6.64	6.89	2.14	1.69

Histological analysis of the vertebrae confirmed the presence of osteolytic tumor within the long bones and vertebrae of the affected animals. Of the twenty animals inoculated with MT-*1luc*+ cells similar results were found. All animals showed localization of bioluminescent signal to the spine or long bones by day 21. However, the bioluminescent signal intensity was quite variable. Nine of the twenty animals had either gross visible tumors or cachexia. Bioluminescent imaging of these animals showed a similar pattern of metastases among these animals. High signal was obtained from the lumbar and thoracic spine, the humerus, femur and tibia in addition to the lung. Micro-CT scans of these animals indicated gross lytic lesions within the vertebral bodies and long bones. Subsequent histological staining with H&E, keratin and immunohistochemical staining for human EGF-r confirmed the presence of human breast cancer cells within the aforementioned sites. FIGURE 9 shows histochemical and immunohistochemical staining of MT-1 cells within vertebrae. A) is H&E staining (10x); B) is Keratin staining (brown) indicating tumor invasion of the bone and bone marrow (5x); C) is Human EGF-r immunohistochemistry (brown) of MT-1 cells within a vertebrae (20x). "T" indicates tumor, while "BM" indicates bone marrow. Four of the animals

had the highest signals within the chest cavity and gross dissection revealed large metastatic tumors within the lung. Six animals showed a diffuse weak bioluminescent signal localized to the thoracic and lumbar spine. Histological confirmation of tumors within the spine was verified in only two of these animals with one animal having metastases identified in the spinal cord. One animal died a few hours following intracardiac tumor injection.

[0027] Determination of the Effect of PDT in Vertebrae and Long Bones with Metastases:

Method: Thirty *rnu/rnu* nude rats were used in this part of the study. The rats received a left ventricular intracardiac injection with MT-1 cells as described earlier. At day 21 post injection each animal was anesthetized with 2% halothane / air mixture and placed on a custom made radiolucent stereotactic jig in the left lateral decubitus position. Prior to this it was established by histological methods that animals with tumors contained tumor in most vertebral bodies and long bones. Because lesions within the vertebral bodies could not be detected by fine detail radiography, T12 and L4 vertebrae were selected as representative levels for treatment. An 18g needle was placed on the cortex of the targeted vertebrae or long bone with the use of a miniC-arm image intensifier. A 300mW diode laser coupled to a 200um fiber was used to deliver 690 nm light. BPD-MA was administered intravenously at a dose of 2mg/kg prior to the administration of the light dose. Drug light intervals included 1 hour, 3 hours and 24 hours. Light doses ranged from 25J to 150J. Light was delivered at 150mW for all treatments and the effects of different drug light intervals and different light doses using a fixed drug concentration were evaluated. The animals were examined for paralysis post treatment. The animals were sacrificed using CO_2 inhalation. Vertebrae were then harvested and fixed in 10% formalin for 7 days. Micro-CT images were obtained and then the samples were decalcified in 10% formic acid for 7 days. The tissue was then blocked and paraffin embedded and 10um sections were cut. The sections were analyzed under light microscopy using H&E staining as well as TUNEL and human EGF-r immunohistochemistry. The area of

effect as denoted by necrosis and apoptosis was identified and measured using a Nikon slide scanner and Image Pro software.

[0028] Targeted Lesions:

Method: Twenty nude *rnu/rnu* (Harlan) female rats (4-6 weeks of age) were used in this part of the study. The protocol was in accordance with the Canadian Council on Animal Care prior to initiation. Prior to injection each animal was anesthetized with 2% halothane / air mixture in a sterile environment. Twenty animals were used for injection. The chest was prepared with alcohol and 2 x10^6 MT-1*luc*+ cells, a human breast cancer cell line carrying the luciferase reporter gene, were injected into the left ventricle using a 1 ml syringe with a 26g needle. Pulsatile blood in the syringe was ensured prior to each injection. The animals were placed back into their cages and fed water and rat chow ad libitum. At day 18 the animals were imaged using the Xenogen IVIS system. To do this 100mg/kg luciferin was injected into the peritoneal cavity of each animal and each animal was imaged 5 minutes following injection for a 1 to 5 minute image acquisition period. The animals were then imaged on the same custom made stereotactic radiolucent jig using a mini-C-arm image intensifier which allowed correlation of the bioluminescent signal to the vertebrae. FIGURE 1 shows stereotactic targeting of bioluminescent metastatic lesions using a mini-C-arm image intensifier. The top left image is a bioluminescent overlay image of a nude rat with metastatic lesions on a radio lucent stereotactic jig. The bottom left image is a fluoroscan image of markers placed along the grid of the stereotactic jig in correlation to the bioluminescent metastases and resulting in localization of the lesion. The bottom right image shows placement of the fiber optic cable sheath (needle cannula) adjacent to the targeted lesion.

The lesions were then targeted and treated with 25J or 150J at a 3 hour drug light interval. The animals were then re-imaged with the Xenogen IVIS system 48 hours post treatment in the stereotactic frame. Signal intensity (photons/second/cm^2) at the targeted site before treatment was compared to

signal intensity following treatment and compared to lesions not treated using Igor Pro software (Alameda, California). The animals were then sacrificed using CO_2 inhalation and the spines and long bones were harvested. Samples were placed in 10% formalin for 7 days and micro-CT images of the vertebrae and long bones were obtained. The vertebrae were examined histologically using H&E staining and immunohistologically with human EGF-r and TUNEL stains as described earlier.

ANOVA Bonferroni and two-tailed paired T-test statistical techniques were applied.

[0029] Determination of the Effect of PDT in Vertebrae with Metastases:

Results: As summarized in TABLE 3, of the thirty animals injected, twenty-five were analyzed.

Table 3. Treatment Groups

	n =	Death Following Tumor Injection	Death Following Verteporfin Injection	Anesthetic Overdose During Imaging / PDT	Death During PDT
MT-1	20	1	1	1	0
MT-1*luc*+	30	1	2	1	1

As summarized in TABLE 4, light doses ranging from 25J to 150J had an ablative effect on both normal bone marrow and tumor tissue. The region of effect ranged from 2.5mm to 22mm in the rostral-caudal dimension.

Table 4. Effect of Different Light Doses on Vertbrae with Metastases

	25J*	50J*	75J*	75J**	100J*	150J*
Area (mm^2)	8.435	15.04	52.38	82.47	45.49	80.53
Rostral-Caudal (mm)	4.59	5.66	11.67	17.47	13.8	13.05
Antero-Posterior (mm)	2.62	3.89	5.09	5.05	5.05	5.78

*Treatment given at drug-light interval of 3 hrs

** Treatment given at drug-light interval of 0.75 hrs

The effect varied in direct proportion to the amount of light given with the greatest effect being seen with 150J. However, a 75J light dose administered at a 1 hour drug light interval produced a similar effect (Table 5).

FIGURE 14 shows brightfield microscopy of H&E sections containing tumor following PDT treatment. A) shows untreated tumor tissue (10x); B) and C) show treated tumor tissue within a vertebral body (10x). FIGURE 15 shows brightfield microscopy of rat vertebrae following PDT treatment. A) shows an H&E section of section of rat spine (the arrows delineate the diameter of the rostral caudal dimension of the area of effect and demonstrate the position of the high powered images in the right column relative to each other. B) shows human EGF-r immunohistochemistry of a contiguous section (2.5x). C) shows TUNEL staining of a contiguous section (2.5x). D) shows H&E of the same section as A), but 10x indicating the boundary of affected and unaffected tumor tissue. E) shows EGF-r immunohistochemistry at the same site as in D) but on a contiguous section (10x). F) shows TUNEL staining at the same site as in D) and E) but on a contiguous section (10x). Histological analysis with H&E of the tissue indicated ablation of the tumor tissue. TUNEL staining of the treated tissue was positive at the periphery of the treatment area while necrosis was predominant centrally.

The use of a custom made stereotactic radiolucent jig facilitated localization and targeted treatment of bioluminescent metastases. FIGURES 10 and 12 show pre and post-PDT treatment bioluminescent imaging of MT-1luc+ metastatic lesions in rnu/rnu rats with BPD-MA. The left column is pre-treatment bioluminescent imaging. In FIGURE 10, the right column is bioluminescent imaging of the animals imaged in the left column 48 hours following PDT treatment with BPD-MA at 150 J with a drug light interval of 3 hours. In FIGURE 12, the right column is bioluminescent imaging of the animals imaged in the left column 48 hours following PDT treatment with BPD-MA at 25 J with a drug light interval of 3 hours. As summarized in FIGURE 11 and TABLE 5a, targeted lesions treated with 150J of light with a 3 hour drug light interval reduced the signal from the targeted site by 87% and decreased tumor growth by 99.8% as compared to control lesions emitted 48 hours following treatment.

Table 5A. Bioluminescent Data

	Mean Count Rx Area	Mean Count UnRx Area	*P* =
Pre-PDT	1.02×10^4	1.98×10^3	< 0.01
Post-PDT	1.42×10^3	1.65×10^5	<0.01
PostRx/PreRx	0.139	83.3	

*for drug light interval of 3 hrs 150J (n = 5)

As summarized in FIGURE 11 and TABLE 5b, targeted lesions treated with 25J of light with a 3 hour drug light interval showed a decrease in tumor growth of 66% compared to that of the control lesions.

Table 5B. Bioluminescent Data

	Mean Count Rx Area	Mean Count UnRx Area	*P* =
Pre-PDT	1.86×10^4	4.05×10^3	<0.05
Post-PDT	2.33×10^4	1.5×10^4	<0.05
PostRx/PreRx	1.25	3.7	

* for drug-light interval of 3 hrs 25 J (n = 2)

No effect was seen when light was administered at a 24 hour drug light interval or in control animals when light alone or drug alone was administered.

As summarized in TABLE 6, hind leg paralysis was seen in animals when treated at the 3 hour drug light interval at T12 at light doses between 50J and 150J but not at 25J. No paralysis was seen at the twenty four hour drug light time interval in animals treated with 150J at T12. No paralysis was seen in animals treated with 150J at the L5 level of the spine. No paralysis was seen in hind legs of rats following treatment with 150J directed at the distal femur.

Table 6. Effect of Light Dose on the Rat Spinal Cord, Spinal Nerves and Peripheral Nerves

Light Energy (J)	Vertebral Level Treated	Drug Light Interval (hr)	Hind Leg Paralysis	*N* =
25	T12	3	0	5
50	T12	3	2 unilateral	5
75	T12	3	1 bilateral	4
100	T12	3	2 unilateral	3
125	T12	3	1 bilateral	2
150	T12	3	3 bilateral	4
150	T12	0.25	4	4
150	T12	24	0	5
150	L4	3	0	5
150	Distal Femur	3	0	3
Control*	T12	3	0	3

* Control – 150J light delivered without drug.

***In vivo* studies in pig model**

[0030] Operative approach:

50 kg pigs were used. The pigs were pre-anesthetized with ketamine/xylazine 20/2mg/Kg IM for induction. An IV line was established and 0.9% saline solution was run at 5 ml/Kg/hr. Verteporfin was administered through the IV line using an infusion pump. The pigs were intubated and maintained on a ventilator with isofluorane / nitrous oxide inhalant by animal care professionals. The pigs were placed prone on a radiolucent surgical table with appropriate bolsters for support and padding. A sterile prep was made with betadine soap and scrub and prep solution. A small stab incision was made over the lumbothoracic spine of the pig.

As shown in FIGURE 16, using a cannulated drill, a customized guide pin was inserted through the incision onto the bone. Placement into the vertebral body through a transpedicular and parapedicular approach was facilitated by the use of a CT-C arm. L1 and L2 vertebrae were targeted.

A cannulated exchange sheath was placed over the guide rod and inserted through the incision. The guide rod was then removed, and a fiber optic cable sheath was then inserted down the cannula of the exchange sheath. A cannulated bone screw assembly, which is described in further detail below, was then placed around the cannulated exchange sheath and inserted through the incision, as shown in FIGURE 17. The cannulated bone screw assembly was pushed down the cannulated exchange sheath. The bone screw assembly comprised a cannulated bone screw, a cannulated locking screw and a flexible, elastometric O-ring. FIGURE 18 shows an expanded view of the cannulated bone assembly (the cannulated bone screw, O-ring and cannulated locking screw) around the cannulated exchange sheath. The cannulated bone screw was secured into bone. In this study, the cannulated bone screw was secured into the pedicle of the vertebral body. The cannulated exchange sheath was then removed, leaving the cannulated bone screw assembly and fiber optic cable sheath behind. The cannulated locking screw was tightened into the head of the bone screw, thus compressing the

O-ring and locking the fiber optic cable sheath in place. A fiber optic cable was passed down the fiber optic cable sheath, as shown in FIGURE 19. FIGURES 20 and 21 show a vertebrae with a bone screw in place and a fiber optic probe inserted.

The detector and diffusing fibers were placed in the same transverse plane. The diffusing fiber was moved incrementally with respect to the detector fiber and differences in power were measured at fiver different distances from the detector source using a computer aided photomultiplier tube.

Hemostasis was maintained with cautery.

690 nm light was delivered into the vertebrae at L1 at light doses ranging from 25 J – 100 J of energy (four animals received one dose of either 25 J, 50 J, 75 J or 100 J and one control animal received no energy). The light dose took into account the optical properties of the 1st and 2nd lumbar vertebrae, such that the does refers to the dose at the site of the bone tumor.

Hemostasis was obtained prior to closure. Closure of the fascia was done with #1 vicryl followed by 2-0 vicryl for the subcutaneous tissue followed by 2-0 proline suture for skin. A sterile bandage was applied over the incision.

The pigs were extubated and allowed activity as tolerated with diet as tolerated.

The pigs were given post-op analgesia (buprenorphine 0.005 – 0.01 mg/Kg IM or carprofen 0.1 – 1 mg/Kg IM) as necessary.

The pigs were observed for development of hindleg paralysis and sacrificed 24 hours post-op if no paralysis occurred. In the even that paralysis occurred, the animal was sacrificed as necessary.

[0031] <u>End points of study:</u>

The end points of the study included: a) in vivo attenuation of 690 nm light in vertebrae; b) observation for hindleg paralysis secondary to the treatment; c) the spinal cord was harvested and examined histologically using H&E staining to determine structural damage from the treatment; and d) a sample of

vertebral body was harvested and imaged with micro-CT to determine the bone density for each vertebral body in which the light attenuation studies were conducted.

[0032] Results:

Five pigs were used in the study. Ten vertebrae were targeted, each vertebrae having two probes placed (one on the right and one on the left side) making for a total of 20 insertions of the customized implantation device.

There was one complication with respect to inserting the guide rod in one vertebrae (1/20) leading to post-operative paresis. One pig developed anaphylactic shock and died, one pig developed anaphylactic shock and was resuscitated and survived without complications. In the other 3 pigs (6 vertebrae) there were no complications. There were no complications attributed to the PDT, for example, no hindleg paralysis.

The use of a CT scan intraoperatively allowed the exact distance between the delivery fiber and the detector fiber to be determined. This enabled the determination of the attenuation of light within the vertebrae, as shown in FIGURES 22 and 23. The treatment of the vertebrae with PDT allowed the area of effect of the treatment to be correlated with the light attenuation data, thus allowing a dose response curve for vertebral bone to be determined. It is anticipated that in humans, a light dosage in the range of 150 J/cm will be used.

The cannulated bone screw and the fibre optic cable sheath may remain in the body for repeated treatments with photodynamic therapy. Once it has been decided not to use PDT treatment at the site of the bone screw anymore, the following method is used. The cannulated locking screw is unlocked and removed from the mammal. The cannulated exchange sheath is reinserted in the mammal around the fiber optic cable sheath. The fiber optic sheath is removed from the mammal. Optionally, the cannulated bone screw is also removed from the mammal. Bone cement is injected through

the cannulated exchange sheath, and the cannulated exchange sheath is slowly removed as the bone cement dries.

[0033] Equipment:

FIGURE 24 shows some of the equipment used in the *in vivo* pig study. At the far right is a fiber optic cable. To the left of the fiber optic cable is a fiber optic cable sheath. To the left of the fiber optic cable sheath is a guide pin. To the left of the guide pin is a cannulated exchange sheath. To the left of the cannulated exchange sheath is a cannulated bone screw assembly.

FIGURE 25 is a drawing of an example of the cannulated bone screw. The cannulated bone screw has a bore, for example, of 2.49 mm diameter. The cannulated bone screw has a frustro conical tip, an externally threaded but internally unthreaded shaft, and a head. The head of the cannulated bone screw has a threaded internal bore of greater diameter than the diameter of the bore of the bone screw. The threaded internal bore of the head ends at a land. The external thread of the shaft is of low torque and high holding since the cannulated bone screw is to be secured into bones that may be weak. Therefore, the external thread of the shaft is a fine thread.

FIGURE 26 is drawing of an example of the cannulated locking screw. The locking screw has a bore through it. The locking screw has an externally threaded shaft. The torque to undo the locking screw is less than the torque to undo the bone screw.

In one embodiment, the bone screw assembly comprises the cannulated bone screw, a flexible elastomeric O-ring and the cannulated locking screw. The O-ring is able to freely pass inside the threads of the internal threaded bore of the head of the bone screw. As the locking screw engages cooperatively with the internal threaded bore of the head of the bone screw, the O-ring contacts the land, thus preventing further axial movement of the O-ring. As the locking screw further engages cooperatively with the internal threaded bore of the head of the bone screw, the O-ring is compressed and deforms radially inward to act as a retainer for the fiber optic cable sheath.

In a second embodiment, no O-ring is used. Rather, the cannulated locking screw has a shaft with slits in it. The head of the bone screw has an inner bore that is wider at the top of the head and narrower internally. As the cannulated locking screw is pushed into the inner bore of the head of the bone screw, the shaft portions of the locking screw are compressed radially inward to act as a retainer for the fiber optic cable sheath.

[0034] While certain features of the invention have been illustrated and described herein, many modifications, substitutions, changes, and equivalents will now occur to those of ordinary skill in the art. For example, the cannulated bone screw and/or cannulated exchange sheath could be used as a conduit to chronically deliver local drugs, such as, for example, chemotherapeutic agents or a PDT drug that is created with low mobility (i.e. doesn't travel through the body). In another example, PDT is also known in the literature to be effective for treating bacterial infections and other conditions. Embodiments of the invention may be used to treat pathologies in the bone, other than bone tumors, with PDT.

[0035] It is, therefore, to be understood that the appended claims are intended to cover all such modifications and changes as fall within the spirit of the invention.

REFERENCES

1. Tombolini, V., et al., *Radiation therapy of spinal metastases: results with different fractionations.* Tumori, 1994. **80**(5): p. 353-6.

2. Walsh, G.L., et al., *Anterior approaches to the thoracic spine in patients with cancer: indications and results.* Ann Thorac Surg, 1997. **64**(6): p. 1611-8.

3. Milker-Zabel, S., et al., *Clinical results of retreatment of vertebral bone metastases by stereotactic conformal radiotherapy and intensity-modulated radiotherapy.* Int J Radiat Oncol Biol Phys, 2003. **55**(1): p. 162-7.

4. Katagiri, H., et al., *Clinical results of nonsurgical treatment for spinal metastases.* Int J Radiat Oncol Biol Phys, 1998. **42**(5): p. 1127-32.

5. Ryu, S., et al., *Image-guided and intensity modulated radiosurgery for patients with spinal metastasis.* Cancer, 2003. **97**(8): p. 2013-8.

6. Fingar, V.H., et al., *Analysis of acute vascular damage after photodynamic therapy using benzoporphyrin derivative (BPD).* Br J Cancer, 1999. **79**(11-12): p.1702-8.

7. Takeuchi, Y., et al., *Induction of intensive tumor suppression by antiangiogenic photodynamic therapy using polycation-modified lipsomal photosensitizer.* Cancer, 2003. **97**(8): p. 2027-34.

8. Rousset, N., et al., *Cellular distribution and phototoxicity of benzoporphyrin derivative and Photofrin.* Res Exp Med (Berl), 2000. **199**(6): p. 341-57.

9. Wiedmann, M., et al., *Neoadjuvant photodynamic therapy as a new approach to treating hilar cholangiocarcinoma: a phase II pilot study.* Cancer, 2003. **97**(11): p. 2783-90.

10. Sutedja, G. and P.E. Postmus, *The role of photodynamic therapy in the management of stage I/II NSCLC.* Lung Cancer, 2001. **34 Suppl 3**: p. S35-8.

11. Hendren, S.K., et al., *Phase II trial of debulking surgery and photodynamic therapy for disseminated intraperitoneal tumors.* Ann Surg Oncol, 2001. **8**(1): p. 65-71.

12. Nathan, T.R., et al., *Photodynamic therapy for prostate cancer recurrence after radiotherapy: a phase I study.* J Urol, 2002. **168**(4 Pt 1): p. 1427-32.

13. Engebraaten, O. and O. Fodstad, *Site-specific experimental metastasis patterns of two human breast cancer cell lines in nude rats*. Int J Cancer, 1999. **82**(2): p. 219-25.

14. Weber, K.L. and M.C. Gebhardt, *What's new in muscculoskeletal oncology*. J Bone Joint Surg Am, 2003. **85-A**(4): p.761-7.

15. Faul, C.M. and J.C. Flickinger, *The use of radiation in the management of spinal metastases*. J Neurooncol, 1995. **23**(2): p.149-61.

16. Wedin, R., H.C. Bauer, and L.E. Rutqvist, *Surgical treatment for skeletal breast cancer metastases: a population-based study of 641 patients*. Cancer, 2001. **92**(2): p. 257-62.

17. Sundaresan, N., et al., *Treatment of neoplastic spinal cord compression: results of a prospective study*. Neurosurgery, 1991. **29**(5): p. 645-50.

18. Rousset, N., et al., *Effects of photodynamic therapy on adhesion molecules and metastasis*. J Photochem Photobiol B, 1999. **52**(1-3): p. 65-73.

19. Richter, A.M., et al., *Photosensitizing efficiency of two regioisomers of the benzoporphyrin derivative monoacid ring A (BPD-MA)*. Biochem Pharmacol, 1992. **43**(11): p. 2349-58.

20. Richter, A.M., et al., *Photosensitizing potency of structural analogues of benzoporphyrin derivative (BPD) in a mouse tumour model*. Br J Cancer, 1991. **63**(1): p. 87-93.

21. Jamieson, C.H., W.N. McDonald, and J.G. Levy, *Preferential uptake of benzoporphyrin derivative by leukimic versus normal cells*. Leuk Res, 1990. **14**(3): p. 209-19.

22. Richter, A.M., et al., *Biodistribution of tritiated benzoporphyrin derivative (3H-BPD-MA), a new potent photosensitizer, in normal and tumor-bearing mice*. J Photochem Photobiol B, 1990. **5**(2): p. 231-44.

23. Gluck, S., et al., *The selective uptake of benzoporphyrin derivative mono-acid ring A (BPD-MA) in differential cell kill of multiple myeloma cells in vitro*. Photochem Photobiol, 1996, **63**(6): p. 846-53.

24. Kurohane, K., et al., *Photodynamic therapy targeted to tumor-induced angiogenic vessels*. Cancer Lett, 2001. **167**(1): p. 49-56.

25. Momma, T., et al., *Photodynamic therapy of orthotopic prostate cancer with benzoporphyrin derivative: local control and distant metastasis*. Cancer Res, 1998. **58**(23): p. 5425-31.

26. Cincotta, L. et al., *Benzophenothiazine and benzoporphyrin derivative combination phototherapy effectively eradicates large murine sarcomas.* Photochem Photobiol, 1996. **63**(2): p. 229-37.

27. Richter, A.M., et al., *Liposomal delivery of a photosensitizer, benzoporphyrin derivative monoacid ring A (BPD), to tumor tissue in a mouse tumor model.* Photochem Photobiol, 1993. **57**(6): p. 1000-6.

28. Takeuchi, A., et al., *A new method of bone tissue measurement based upon light scattering*. J Bone Miner Res, 1997. **12**(2): p. 261-6.

29. Casas, A., et al., *In vitro photosensitisation of a murine mammary adenocarcinoma cell line with Verteporfin*. Cell Mol Biol (Noisy-le-grand), 2002. **48**(8): p. 931-7.

30. Rehemtulla, A., et al., *Rapid and quantitative assessment of cancer treatment response using in vivo bioluminescence imaging*. Neoplasia, 2000. **2**(6): p. 491-5.

31. Wetterwald, A., et al., *Optical imaging of cancer metastasis to bone marrow: a mouse model of minimal residual disease*. Am J Pathol, 2002. **160**(3): p. 1143-53.

I claim:

1. The use of photodynamic therapy for ablating cells of a tumor located on or in a bone.

2. A method comprising:

inserting a guide rod through an incision into a bone of a mammal;

placing a cannulated exchange sheath over the guide rod;

removing the guide rod;

inserting a fiber optic cable sheath in the cannula of the cannulated exchange sheath so that a proximal end of the fiber optic cable sheath is at or in the bone and a distal end of the fiber optic cable sheath is accessible;

placing a screw assembly around the cannulated exchange sheath, the screw assembly including a cannulated bone screw and a cannulated locking screw;

securing the cannulated bone screw into the bone;

removing the cannulated exchange sheath from the mammal; and

fixing the cannulated locking screw into a head of the cannulated bone screw, thus securing the fiber optic cable sheath to the cannulated bone screw.

3. The method of claim 2, further comprising:

inserting an optical fiber cable in the fiber optic cable sheath to enable the delivery of light to the bone.

4. The method of claim 3, further comprising:

administering a photosensitizing drug to the mammal; and

delivering light to the bone via the optical fiber cable to ablate tumor cells in the bone.

5. The method of claim 2, further comprising:

placing the cannulated exchange sheath over the fiber optic cable sheath;

unlocking the cannulated locking screw;

removing the fiber optic cable sheath from the mammal;

injecting bone cement through the cannula of the cannulated exchange sheath into the bone; and

removing the cannulated exchange sheath from the mammal as the bone cement dries.

6. The method of claim 5, further comprising:

removing the cannulated bone screw from the mammal prior to injecting bone cement through the cannula of the cannulated exchange sheath.

7. A cannulated bone screw comprising:

a frustro conical tip having a bore along its axis of rotation;

an externally threaded, internally unthreaded shaft having a bore along its axis; and

a head having a threaded internal bore,

wherein the external thread of the shaft is of low torque and high holding.

8. A cannulated bone screw assembly comprising:

a cannulated bone screw including:

a frustro conical tip having a bore along its axis of rotation;

an externally threaded, internally unthreaded shaft having a bore along its axis; and

a head having an internal bore that is threaded for at least a portion of the internal bore,

wherein the external thread of the shaft is of low torque and high holding;

a flexible O-ring; and

a cannulated locking screw including:

a head having a bore; and

an externally threaded shaft to engage cooperatively with the threaded internal bore of the head of the cannulated bone screw.

Application number / numéro de demande: 2446663

Figures: 1, 2, 4, 5, 6, 7, 8, 9, 10, 11, 12a, b, c, d, 13, 14, 15, 16, 17, 18, 19, 20

Pages: 21, 23, 24,

Unscannable items
received with this application
(Request original documents in File Prep. Section on the 10th floor)

Documents reçu avec cette demande ne pouvant être balayés
(Commander les documents originaux dans la section de préparation des dossiers au 10ème étage)

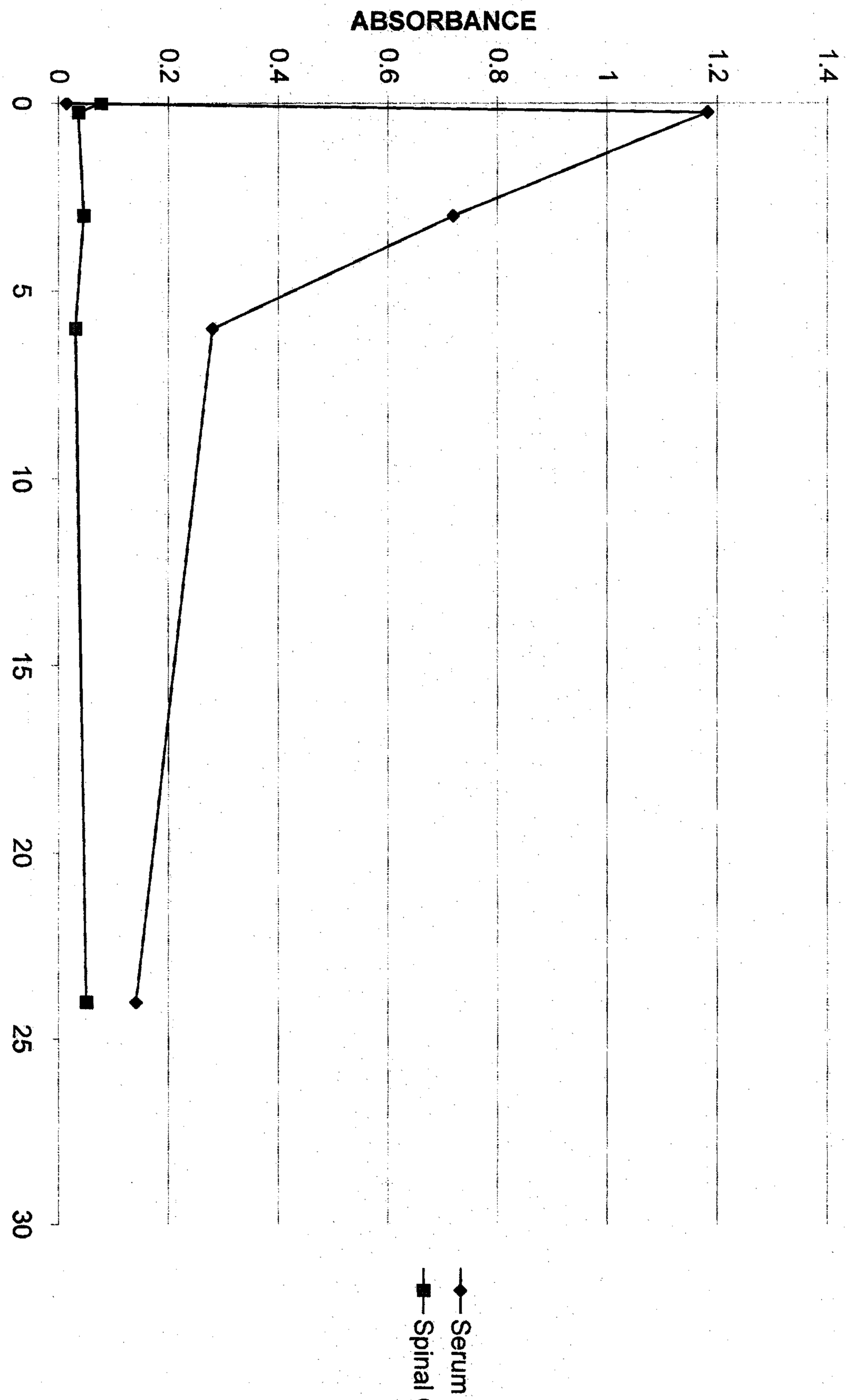


FIGURE 3. BPD-MA DRUG UPTAKE IN SERUM AND SPINALCORD OF THE NUDE RAT

CA 02446663 2003-10-24

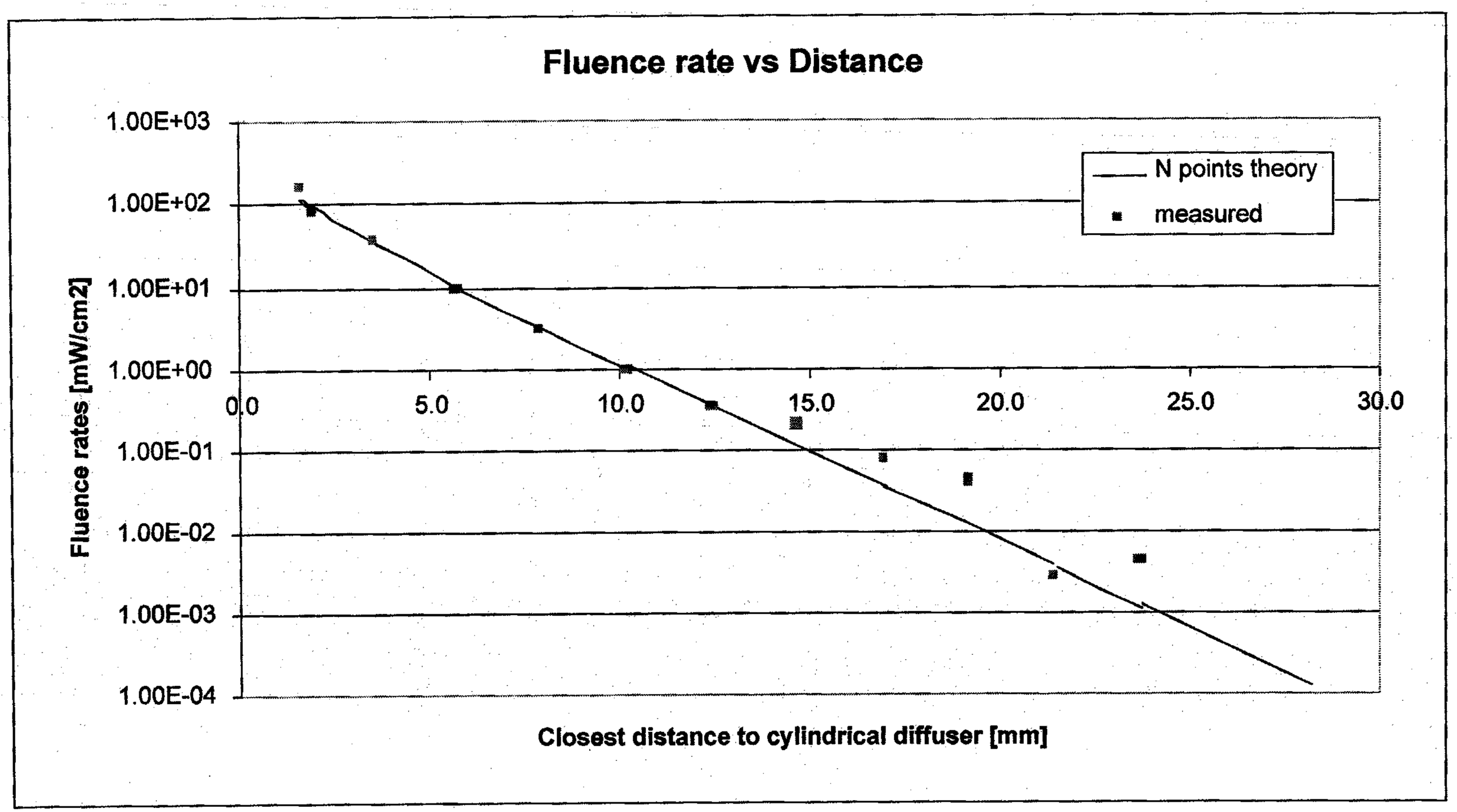
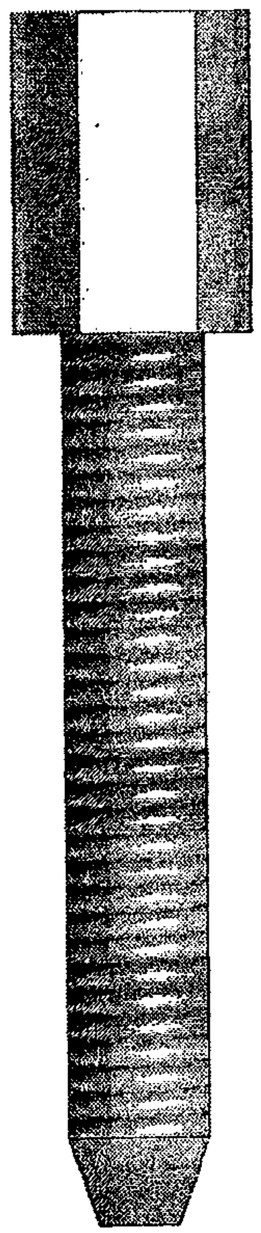
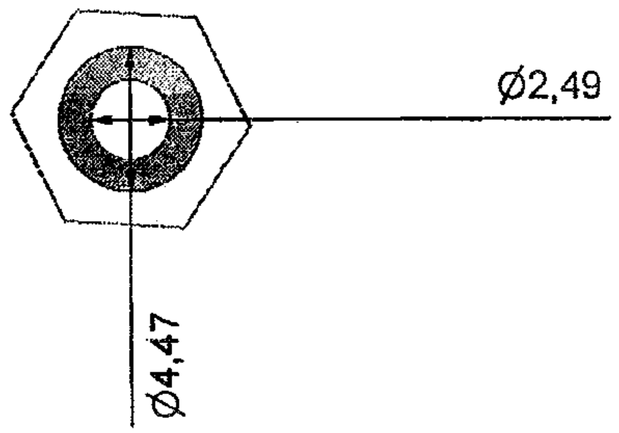
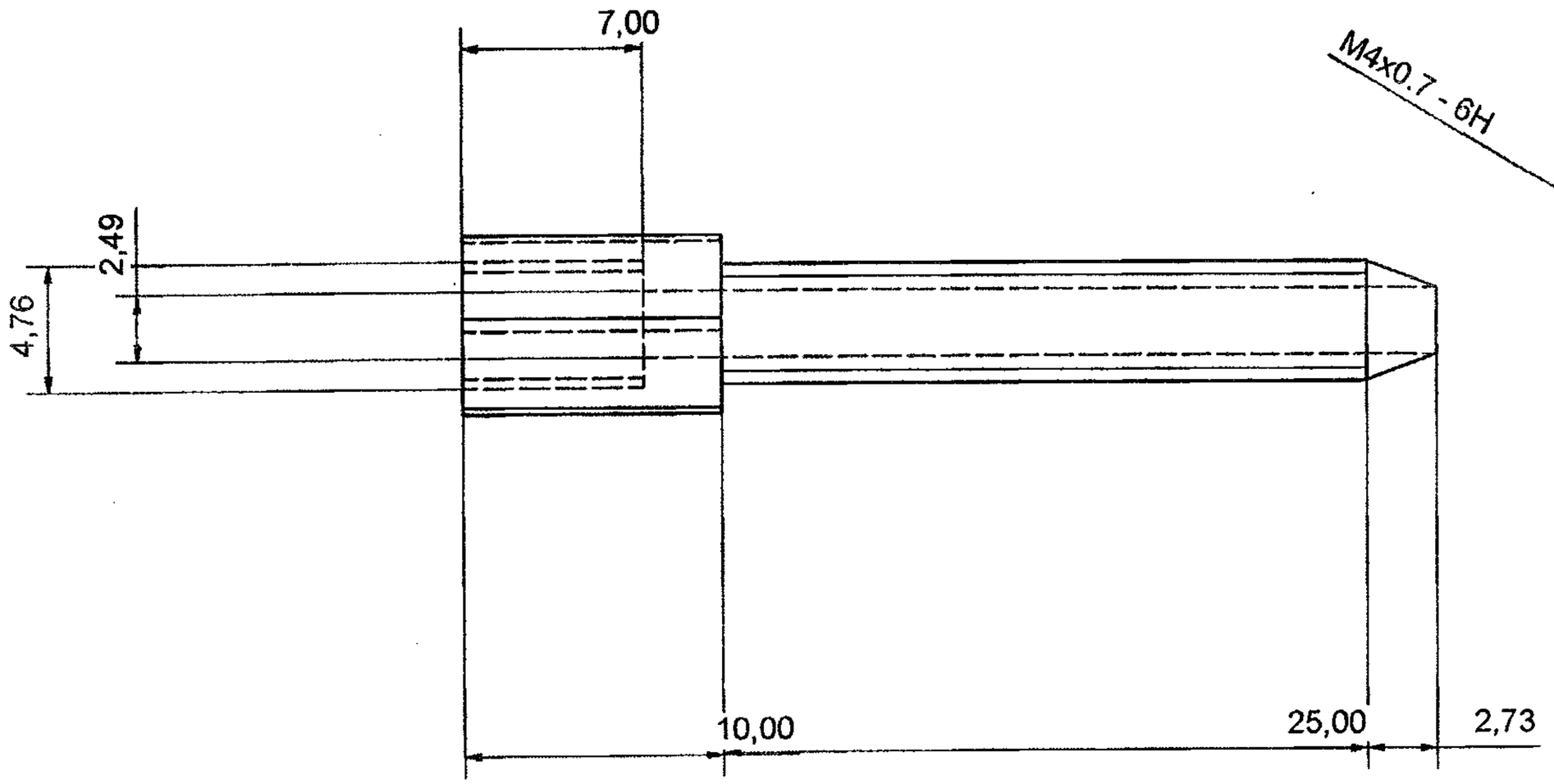


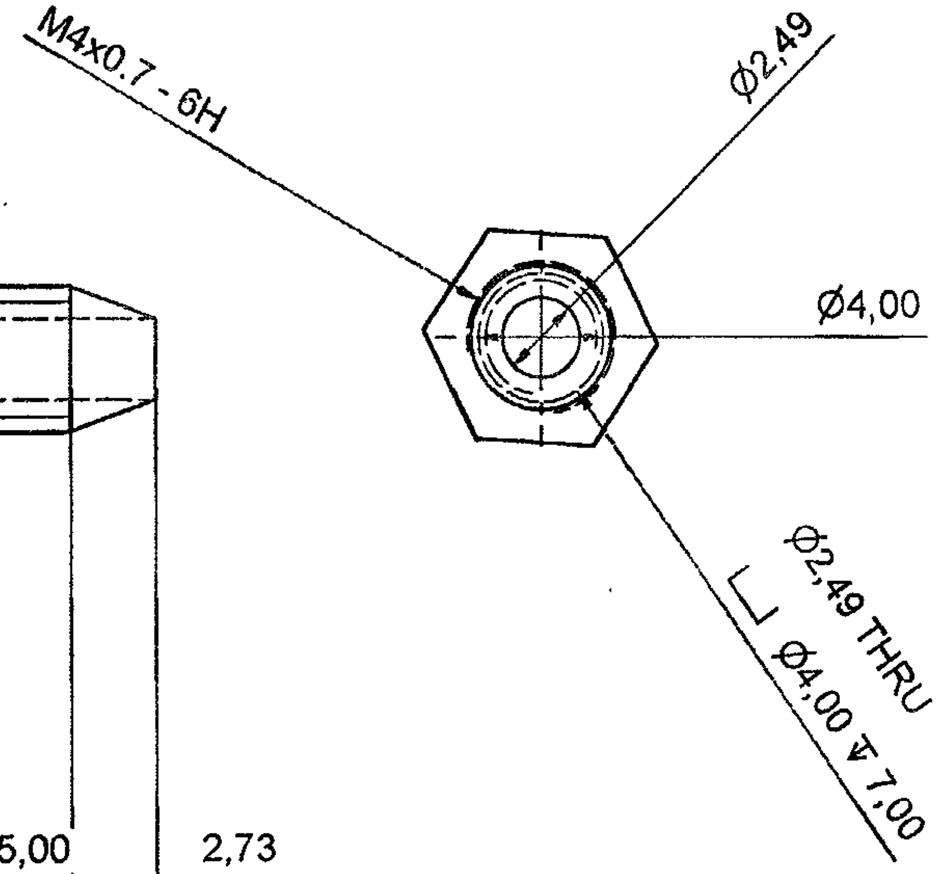
FIGURE 22

FIGURE 25







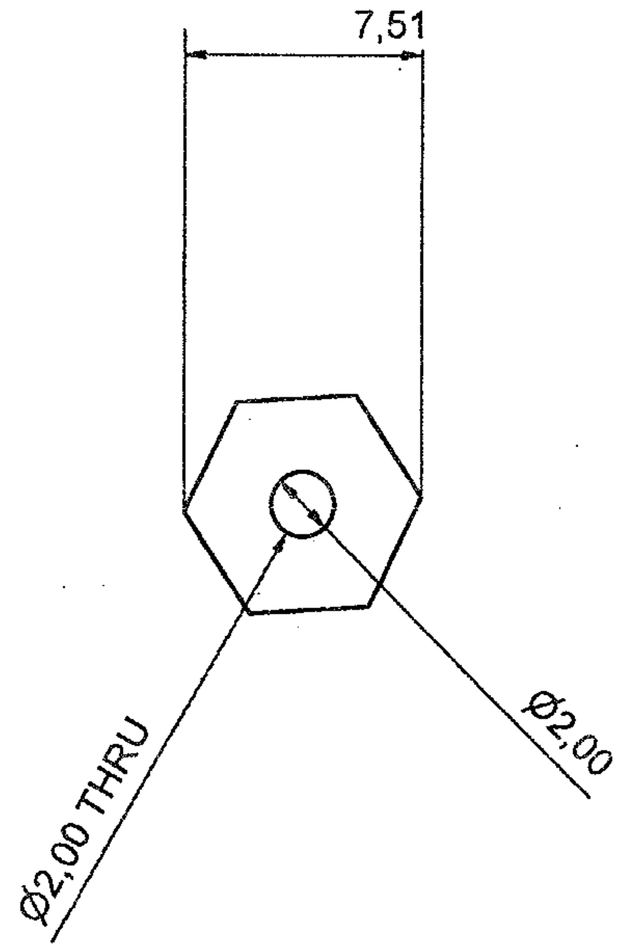


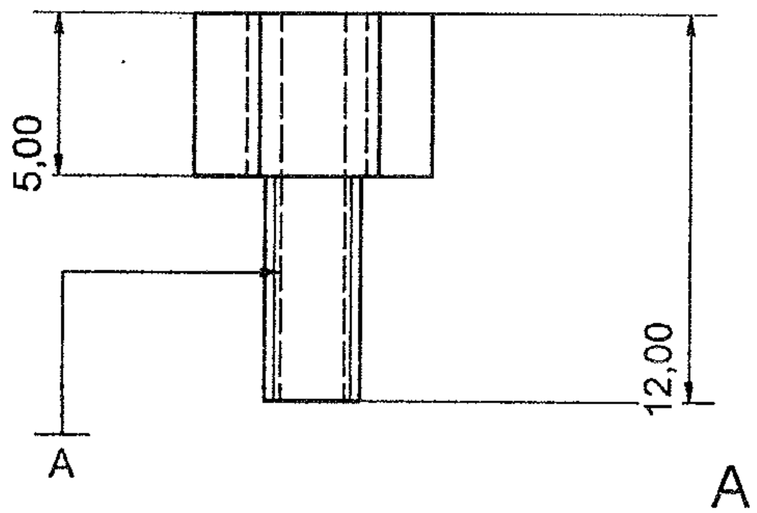
CA 02446663 2003-10-24

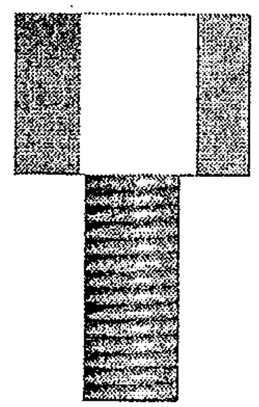
Designed by	Checked by	Approved by - date		Date	
Shane Burch				10/04/2003	

	Edition	Sheet
		1 / 1

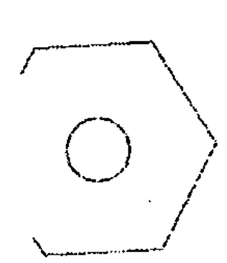
FIGURE 26

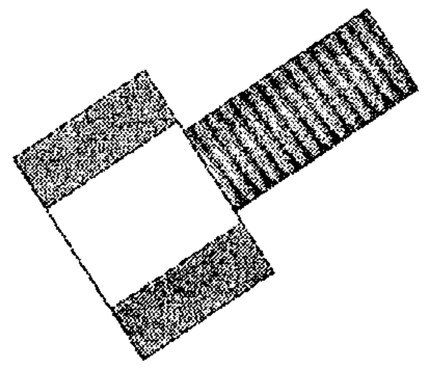






A (4 : 1)





Designed by	Checked by	Approved by - date		Date	
Shane Burch				10/04/2003	

	Edition	Sheet
		1 / 1

CA 02446663 2003-10-24